

Melamine-based Functionalized Graphene Oxide and Zirconium Phosphate for High Performance Removal of Mercury and Lead Ions from Water

Ayyob M. Bakry^{†‡}, Fathi S. Awad^{†§}, Julian A. Bobb[†], Amr A. Ibrahim^{†§}, and M. Samy El-Shall^{†*}

[†]Department of Chemistry, Virginia Commonwealth University, Richmond, VA 23284, USA

[‡]Department of Chemistry, Faculty of Science, Jazan University, Jazan 45142, Saudi Arabia

[§]Chemistry Department, Faculty of Science, Mansoura University, Mansoura 35516, Egypt

Supporting Information

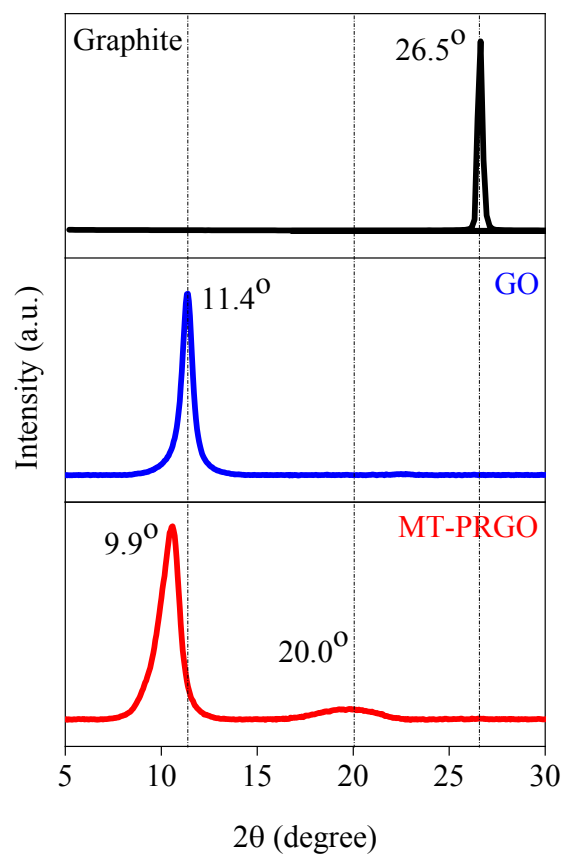


Figure S1. XRD patterns of Graphite, GO, and MT-PRGO.

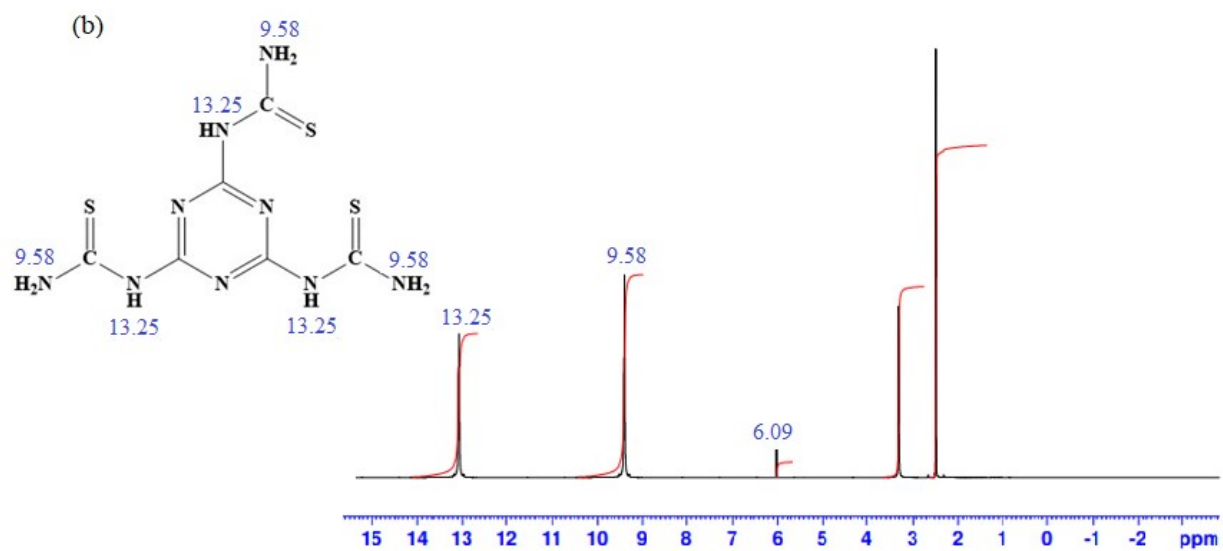
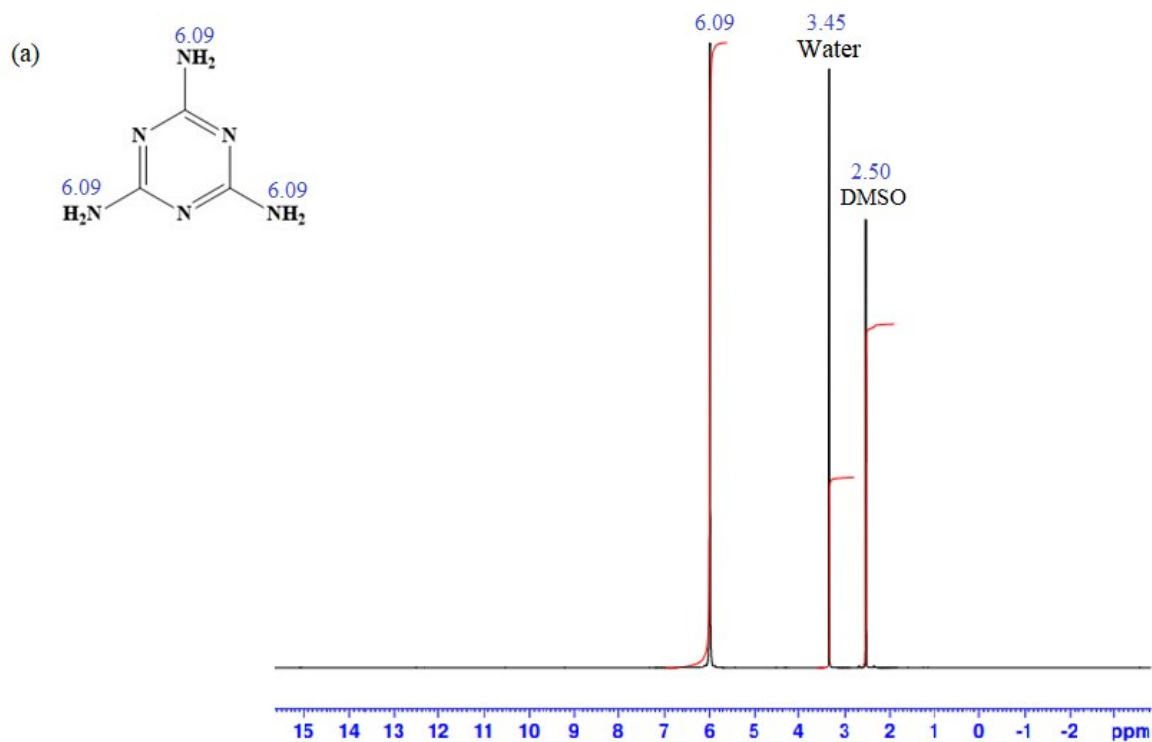


Figure S2. ¹H NMR spectra of (a) melamine and (b) melamine thiourea (MT).

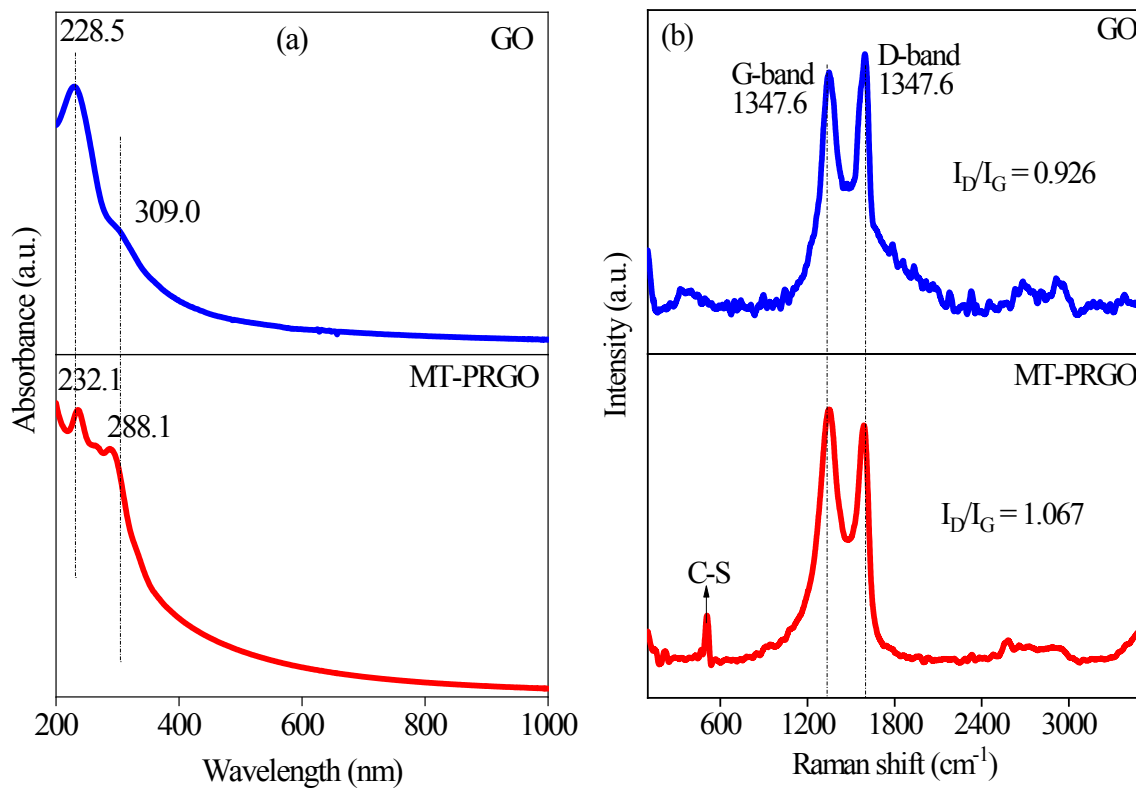


Figure S3 (a) UV-Vis and (b) Raman spectra of GO and MT-PRGO.

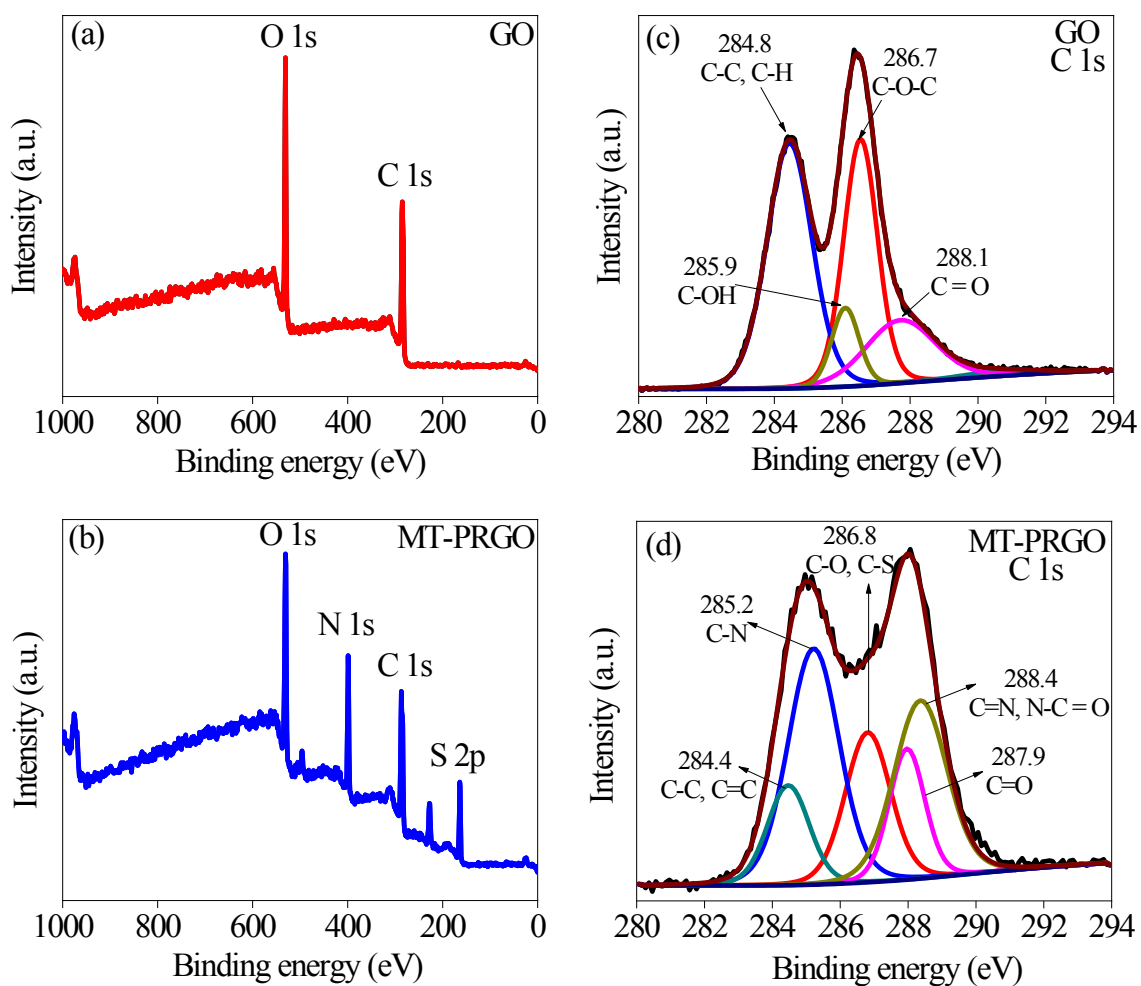


Figure S4. (a & b) XPS survey spectra, (c & d) C 1s of GO and MT-PRGO.

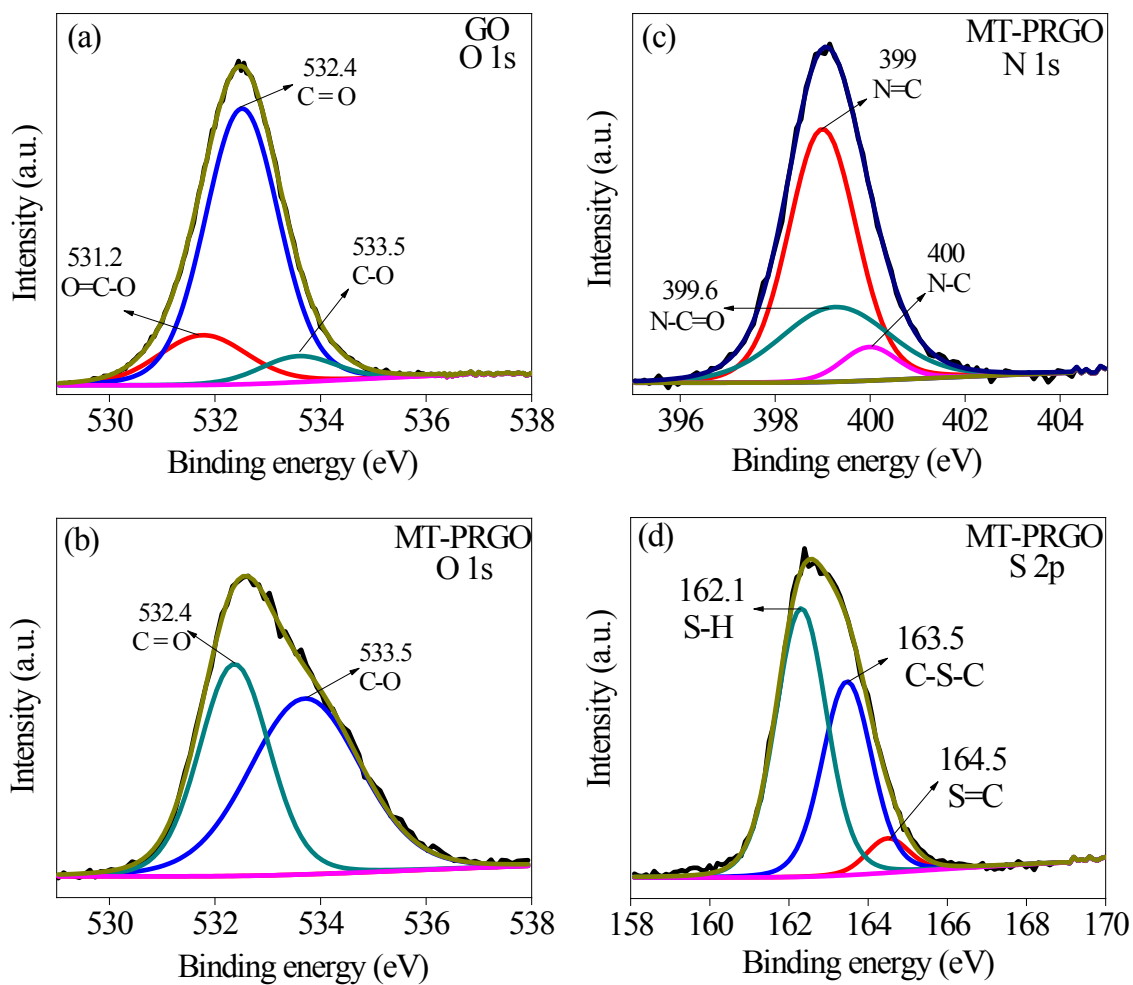


Figure S5. XPS spectra of (a & b) O 1s for GO and MT-PRGO, (c) N 1s, and (d) S 2p of MT-PRGO.

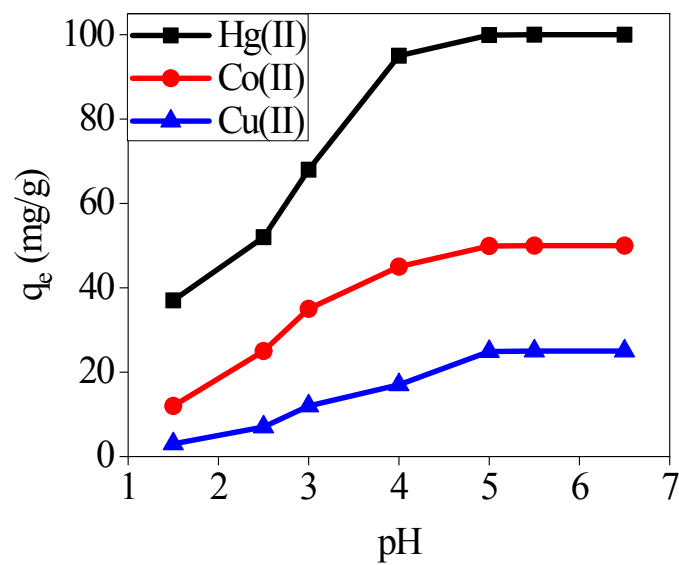


Figure S6. The effect of pH on the removal of Hg(II), Co(II), and Cu(II) ions by the MT-PRGO adsorbent [conditions: $C_0 = (100, 50, 25 \text{ mg/g})$, respectively, $T = 298 \text{ K}$; adsorbent dose = 0.005 g/5 mL , $t = 6 \text{ h}$].

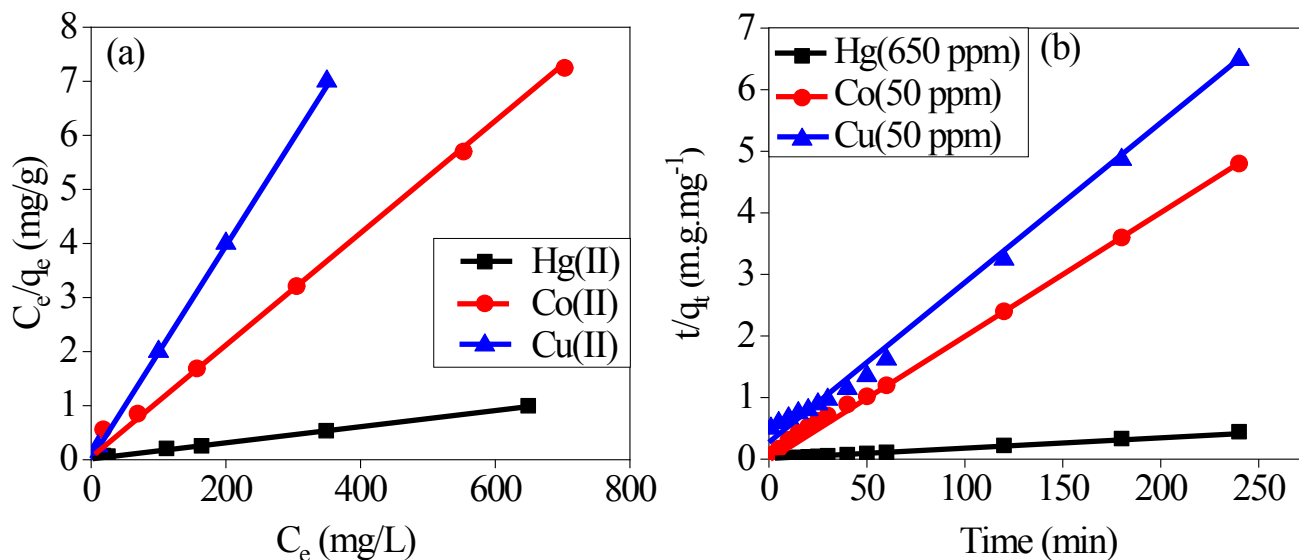


Figure S7. Langmuir isotherm model for the adsorption of Hg(II), Co(II), and Cu(II) ions on MT-PRGO. (B) Pseudo-second-order kinetic model for the adsorption Hg(II), Co(II), and Cu(II) ions on MT-PRGO.

Table S1. Parameters of the Langmuir isotherms model for the adsorption of Hg(II), Co(II), and Cu(II) ions on MT-PRGO.

Metal ion	R ²	b (L/mg)	Q _{max, fitted}	Q _{exp}	R _L
Hg(II)	0.997	0.096	661.0	651.0	0.0079
Co(II)	0.995	0.080	98.8	98.0	0.0153
Cu(II)	0.994	0.044	50.1	50.0	0.0537

Table S2. Kinetic parameters for the adsorption of Hg(II), Co(II) and Cu(II) ions on MT-PRGO.

Metal ion	q _{e, exp} (mg g ⁻¹)	q _{e, calc} (mg g ⁻¹)	k ₂ (g mol ⁻¹ min ⁻¹)	R ²
Hg(II)	538.0	543.2	0.001218	0.997
Co(II)	48.8	51.3	0.004029	0.998
Cu(II)	40.1	39.5	0.002211	0.993

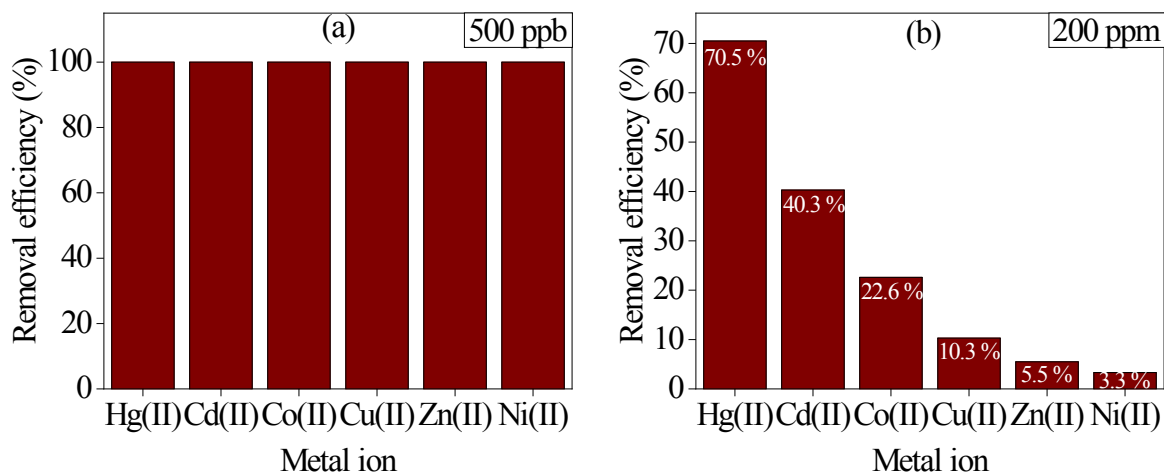


Figure S8. The effect of competitive ions on the removal of a mixture of toxic metals by MT-PRGO (a) $C_0 = 500 \mu\text{g/L}$, (b) $C_0 = 200 \text{ mg/L}$ [conditions: adsorbent dose = 0.05 g/ 5 mL, pH = 5.5, T = 298 K].

Table S3. Adsorption capacities of MT-PRGO in mixed metal ions system 500 ppb and 200 ppm at pH 5.5.

Concentration	Metal ion	Hg(II)	Cd(II)	Co(II)	Cu(II)	Zn(II)	Ni(II)
500 $\mu\text{g/L}$	C_e (mg/L)	0	0	0	0	0	0
	q_e ($\mu\text{g/g}$)	500.0	500.0	500.0	500.0	500.0	500.0
200 mg/L	C_e (mg/L)	59.0	120.0	155.0	179.0	189.0	193.3
	q_e (mg/g)	141.0	80.0	40.0	21.0	11.0	6.7

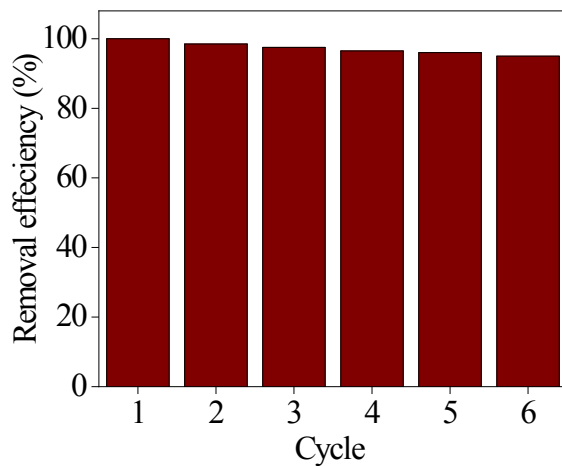


Figure S9. Recycling of MT-PRGO for the removal of Hg(II) [desorption condition: 1.0 M HNO₃, adsorption conditions: pH 5.5, dose: 1 g/L, initial concentration of Hg (II) = 250 mg/L].

Table S4. Desorption studies of Hg(II) from MT-PRGO using HNO₃.

Metal	Eluent	q _e Adsorbed (mg/g)	q _e Desorbed (mg/g)	De (%)
250 mg/L Hg(II)	HNO ₃ (0.5 M)	232.0	135.5	58.40
	HNO ₃ (1.0 M)	232.0	155.2	66.89
	HNO ₃ (1.5 M)	232.0	221.2	95.34
	HNO ₃ (2.0 M)	232.0	232.0	100.00

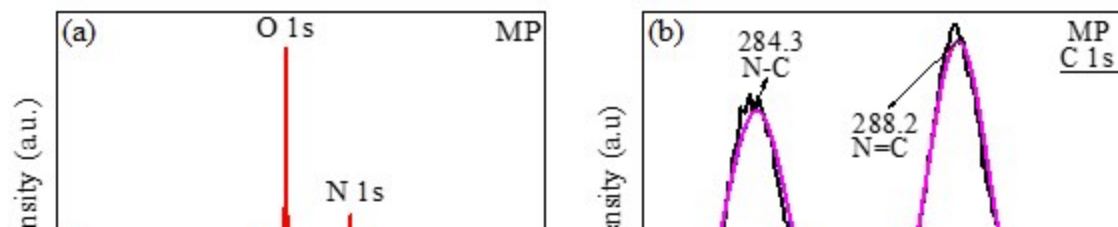


Figure S10. XPS spectra of MP (a) Survey scan, (b) C 1s, (c) N 1s, (d) P 2p, and (e) O 1s.

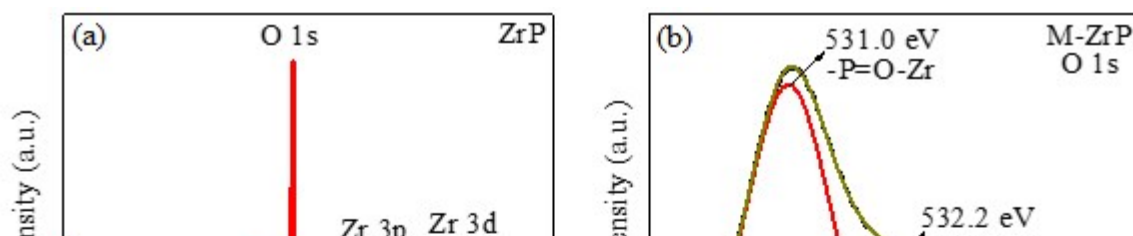


Figure S11. XPS spectra of ZrP (a) Survey scan, (b) O 1s, (c) P 2p, and (d) Zr 3d.

Table S5. Surface elemental composition of MP and M-ZrP from XPS analysis.

Adsorbent	Elemental Content (%)				
	C _{1s}	N _{1s}	O _{1s}	P _{2p}	Zr _{3d}
MP	10.8	24.1	49.3	15.8	0.0
ZrP	0.0	0.0	57.2	20.3	22.5
M-ZrP	8.8	22.9	40.9	15.6	11.9

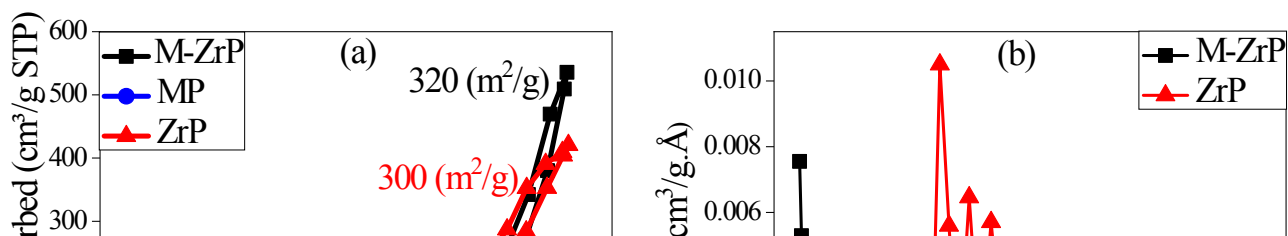


Figure S12. (a) N₂ adsorption-desorption isotherms of MP, ZrP, and M-ZrP. (b) Estimated pore size distributions of ZrP and M-ZrP.

Table S6. BET surface area and estimated pore volume of MP, ZrP and M-ZrP.

Sample	Surface area (m ² /g)	Pore volume (cm ³ /g.Å)
MP	9	-
ZrP	300	0.010
M-ZrP	320	0.008

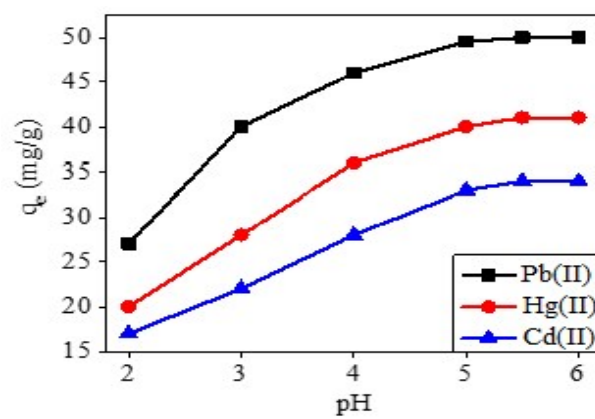


Figure S13. Dependence of the M-ZrP adsorption capacity of Pb(II), Hg(II), and Cd(II) ions on the pH of the solution [conditions: $C_0 = 50 \text{ mg/L}$ $T = 298 \text{ K}$; adsorbent dose = 0.005 g/5 mL].

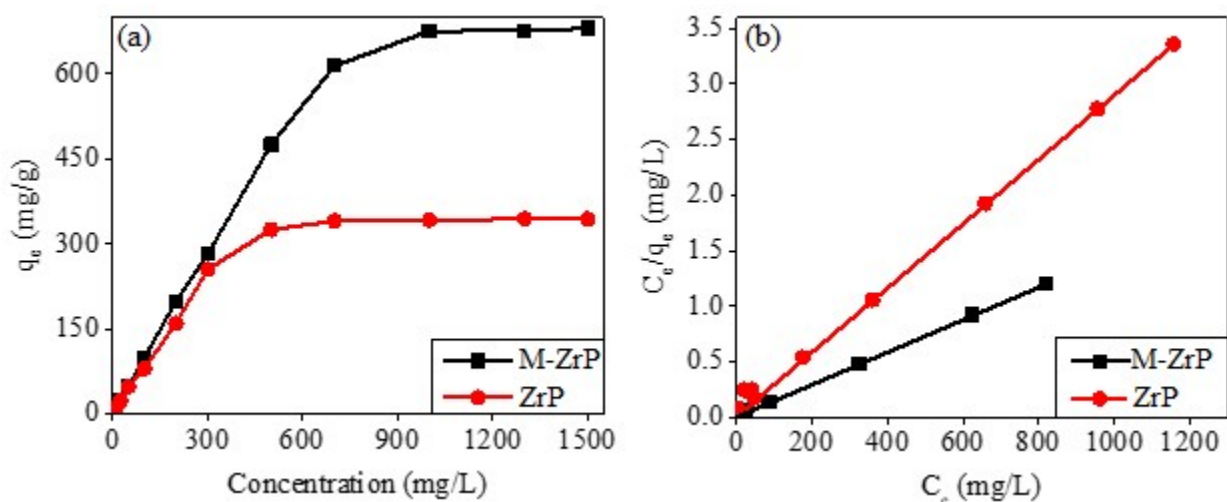


Figure S14. (a) Comparison of the removal of Pb(II) by the ZrP and M-ZrP adsorbents [Conditions: $C_0 = 10 - 1500 \text{ mg/L}$ Pb(II), pH 5.5, $T = 298 \text{ K}$, adsorbent dose = 0.005 g/5 mL]. **(b)** Langmuir isotherm model for the adsorption of Pb(II) on ZrP and M-ZrP. The parameters of the Langmuir-isotherms for the adsorption of Pb(II) on ZrP and M-ZrP are shown below.

Langmuir parameters					
Adsorbent	R^2	$b \text{ (L/mg)}$	$Q_{\text{max, fitted}}$	Q_{exp}	R_L
M-ZrP	0.993	0.164	682.6	680.4	0.0041
ZrP	0.997	0.024	348.3	344.2	0.0400

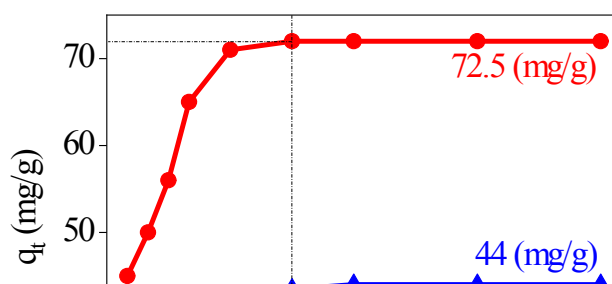


Figure S15. Effect of contact time on the removal of Hg(II) and Cd(II) ions by M-ZrP [Conditions: $C_0 = 100$ mg/L, pH = 5.5; T = 298 K; adsorbent dose = 0.005 g/5 mL].

Table S7. Desorption studies of Pb(II), Hg(II) and Cd(II) from M-ZrP using different concentrations of nitric acid.

Metal	Eluent	q_e Adsorbed (mg/g)	q_e Desorbed (mg/g)	D_e (%)
1000 mg/L Pb(II)	HNO ₃ (0.1 M)	672.0	564.0	83.92
	HNO ₃ (0.5 M)	672.0	584.0	86.90
	HNO ₃ (1.0 M)	672.0	646.0	96.13
	HNO ₃ (1.5 M)	642.0	642.0	100.0
300 mg/L Hg(II)	HNO ₃ (0.1 M)	108.0	78.0	72.22
	HNO ₃ (0.5 M)	108.0	90.0	83.33
	HNO ₃ (1.0 M)	108.0	98.0	90.74
	HNO ₃ (1.5 M)	108.0	108.0	100
300 mg/L Cd(II)	HNO ₃ (0.1 M)	56.0	37.5	66.96
	HNO ₃ (0.5 M)	56.0	44.7	79.82
	HNO ₃ (1.0 M)	56.0	53.0	94.64
	HNO ₃ (1.5 M)	56.0	56.0	100

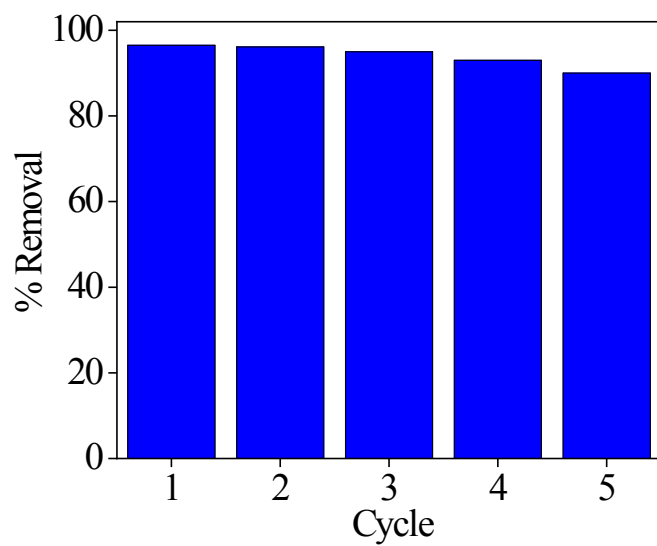


Figure S16. Recycling of M-ZrP adsorbent for the removal of Pb(II) (desorption condition: 1.5 M HNO₃) [adsorption conditions: pH 5.5, dose = 1 g/L, initial concentration of Pb (II) = 1000 mg/L].

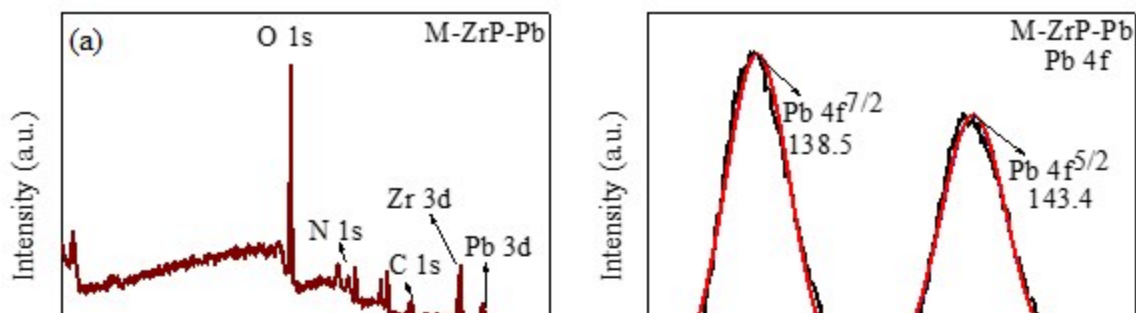


Figure S17. XPS spectra of M-ZrP after the adsorption of Pb(II) ions. (a) Survey scan and high resolution spectra of (b) Pb 4f, (c) C 1s, (d) Zr 3d (e) N 1s, and (f) O 1s electrons.